Low-Dimensional Solids: An Interface between Molecular and Solid-State Chemistry? The Example of Chainlike Niobium and Tantalum Chalcogenides

J. ROUXEL

Institut des Matériaux, UMR CNRS No. 110, Université de Nantes, 2, rue de la Houssinière, 44072 Nantes Cedex 03, France

Received January 3, 1992

Solids bring to mind the idea of volume, and it may therefore seem paradoxical to discuss solids of "low dimensionality". This concept, however, is quite relative and in fact refers to situations in which the chemical bonding exhibits a high degree of directional anisotropy. A low-dimensional solid is, on a microscopic scale, composed of stacked sheets or juxtaposed fibers. Strong ionic/covalent or metallic bonds exist within the sheets or fibers, while only weak interactions, most often van der Waals forces, exist between them. This bonding combination is responsible for the lamellar (or fibrous) morphologies of certain well-known, naturally-occurring crystals such as mica, graphite, and molybdenite (or asbestos).

A more quantitative characterization of low-dimensional solids takes advantage of the anisotropy of a certain physical property, which directly illustrates the anisotropy in the chemical bonding. To a large extent, the attention given to low-dimensional solids is also related to such an anisotropy which can induce, for example, lubricating properties. The great interest devoted to the physics of low-dimensional compounds during the past 20 years, however, is largely due to the fact that the properties of such materials, lamellar for example, cannot be fully described by simply translating into two dimensions the laws governing three-dimensional space. The resulting properties are different, often totally new. This is the case with low-dimensional magnetism or, more typically, with charge density waves, which are coupled fluctuations of electronic density and atomic positions along a conducting chain or layer.[1-3]

One can consider that low-dimensional solids are the result of a condensation of infinite planar or linear molecules. This point of view establishes a common ground between solid-state and molecular chemistry, notably coordination chemistry. A solid-state magnetic chain is indistinguishable from those prepared by coordination chemists. The boundaries between the fields, sometimes artificially created by their respective names, vanish in light of the concepts and language obviously common to both. It is also worth noting that low-dimensional solids are stable for rather low bond ionicities between metal and nonmetal elements, which gives a great importance to orbital descriptions and reinforces the proximity to coordination chemistry.

Jean Rouxel is a professor at the Institut Universitaire de France. He was born in Brittany in 1935 and received his undergraduate education at the University of Rennes. He received his doctorat d'Etat in Sciences in 1961 at the University of Bordeaux. In 1963 he moved to the newly opened University of Nantes and founded the Laboratory of Solid State Chemistry. He became a full professor in 1972. His research concerns the design and characterization of low-dimensional solids with the concepts of soft solid-state chemistry and the discovery and investigation of the extraordinary properties of inorganic chains and charge density waves.

In addition, layered and chain compounds also have fascinating chemical reactivities,[4] lending themselves to redox interaction–desintercalation processes, pillaring reactions, and acid–base chemistry involving a condensation of parts of the framework to obtain related, but new, structures.

The synthesis of new low-dimensional solids relies on difficult chemistry that simultaneously takes into account many different factors, some of them largely conflicting. The design of chainlike niobium and tantalum chalcogenides reported here illustrates the experimental approaches that can be used to stabilize chainlike arrangements or to strengthen low-dimensional character when starting from a given compound.

Some Preliminary General Considerations

Close inspection of low-dimensional solids leads one to notice that the constituent sheets or fibers most of the time are the result of the condensation of polyhedra composed of a metal surrounded by nonmetal atoms. Edge-sharing [TiS_6] octahedra thus generate "octahedral" TiS_2 layers that are often compared to [STiS] sandwiches. Most often, similar anionic layers (here S^{2-} layers) are facing each other along the van der Waals gap. This example illustrates two crucial points.

(i) In a chemical formula MX_n with a rather high nonmetal content, the value of n increases with decreasing dimensionality. This is a direct consequence of the arrangement of polyhedra with an increasing number of unshared edges or corners to form slabs or fibers.

(ii) Similar anionic layers repel each other, and this excludes the formation of low-dimensional solids for highly ionic structures. If a low-dimensional framework is stable, tuning of the bond ionicity controls the magnitude of the interlayer repulsion. The more ionic the materials, the stronger the tendency to exhibit low dimensionality through anion–anion repulsion (with separation of the sheets and/or fibers), but the less stable the structure. It can be said that the limit of low dimensionality is the intrinsic instability that it generates. Therein lies the difficulty of the synthesis of these phases, which can rely only on qualitative approaches.

Low-dimensional solids are not usually found in the chemistry of oxides and fluorides because these compounds are too ionic. The stabilization of layered arrangements in oxides requires specific conditions. They

(1) Gorkov, L. P.; Grüner, G. In *Charge Density Waves in Solids*; North-Holland: Amsterdam, 1989.
(2) Wilson, J. A.; DiSalvo, F. F.; Mahajan, S. *Adv. Phys.* **1975**, *24*, 117.
(3) Rouxel, J. In *Crystal Chemistry and Properties of Materials with Quasi 1D-Structures*; D. Reidel: Dordrecht, The Netherlands, 1986; p 205.
(4) Rouxel, J. *Chem. Scr.* **1988**, *28*, 33.

0001-4842/92/0125-0328$03.00/0

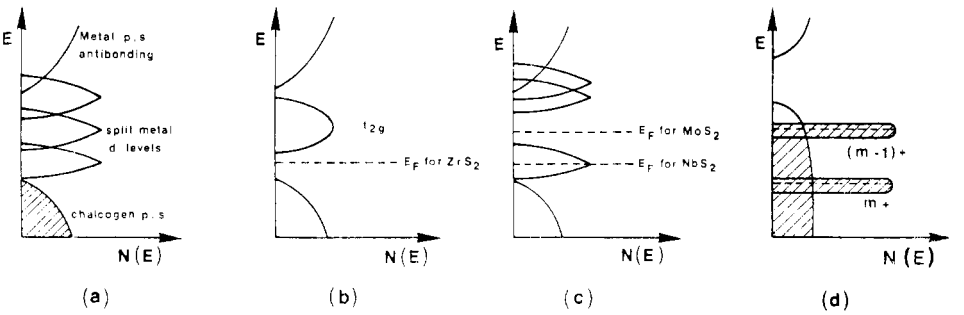

Figure 1. Simplified band models for layered chalcogenides: (a) general scheme; (b) octahedral slabs; (c) trigonal prismatic slabs; (d) cationic levels and sp anionic band at the end of a period.

can be observed in the following cases.

(i) The highest oxidation states of transition metals. For such cases, a strong polarization of the electrons of the anions toward the inside of the slabs exists. This is well illustrated by MoO_3 and, to some extent, by V_2O_5.

(ii) Systems where there is a partial or total protonation of the slabs. Protonation reduces the overall charge on the layers and allows the formation of stabilizing hydrogen bonds across the van der Waals gap. This is the case for layered hydroxides such as brucite, $Mg(OH)_2$, and for many silicates.

(iii) Compounds containing cations located between the sheets, separating negative layers and introducing a favorable term in the energy of the system. Na_xMO_2 derivatives that are isostructural with the Na_xMS_2 intercalation compounds have been prepared, even though there is no corresponding layered MO_2 oxide.[5]

Yet other interesting examples, dominated by mixed polyhedral structural arrangements, are found in the silicate family. In layered silicates, $[SiO_4]$ tetrahedra are always located at the surface of a composite slab; the interior sections of the sheets, if there are any, are composed of octahedra, usually AlO_6 or MgO_6. Indeed tetrahedra, containing the shortest anion–cation distances, permit a strong polarization of the electronic density and a stabilization of the structure. This phenomenon is well illustrated in the recently prepared layered phosphatoantimonic acids and salts, compounds consisting of internal rings of $[SbO_6]$ octahedra capped by external $[PO_4]$ tetrahedra.[6]

A convenient way to obtain layered or one-dimensional arrangements is to decrease the ionicity of the bonds by working, for example, with sulfides, selenides, or tellurides instead of oxides. This evolution favors the stability of low-dimensional arrangements. On the other hand, it brings about new problems that may arise from a redox competition now made possible between cationic d orbitals and anionic sp hybrid orbitals. This interaction can easily be understood by considering the classical band scheme for transition-metal chalcogenides (Figure 1a–c). Between a valence band that is essentially a ligand sp in character and antibonding levels that originate mostly from the corresponding cationic sp levels, the d orbitals of the metal, split by the crystal field, play an essential role in determining the physical properties. Additionally, they govern the stability, and even the stoichiometries, of layered structures. In the presence of sulfur, a maximum cationic oxidation state of four is observed, leading to a d^0 configuration and no electronic conductivity in the case of group IVA elements. The octahedral environment of the metal results in a broad, empty t_{2g} conduction band. For V, Nb, and Ta, a d^1 configuration leads to the lower symmetry trigonal prismatic coordination. The associated band structure is composed of a narrow a'_1 band below the e′ and e″ bands. The a'_1, mostly comprised of metal d_{z^2} orbitals, is lower in energy than the t_{2g}. The result is a net stabilization and metallic behavior. Next, with a d^2 configuration and the same symmetry, MoS_2 and WS_2 are diamagnetic semiconductors. Further to the right, a return to octahedral symmetry for layered MnS_2 is expected (no stabilization through a trigonal prismatic distortion for a d^3 configuration), but that phase cannot be obtained. In fact, for metals further to the right of the periodic table, the d levels are progressively lower in energy and overlap with the sp valence band. Under such conditions, empty d levels are filled at the expense of the valence band, at the top of which holes appear (Figure 1d). In other words, the cation is reduced and the anion is oxidized via the formation of anionic pairs. As a result, layered structures (such as TiS_2, with Ti^{4+} and $2S^{2-}$) becomes pyrites and marcasites (with Fe^{2+} and $(S_2)^{2-}$, for example). Because selenium is less electronegative than sulfur, the top of the sp valence band in metal diselenides is situated at a higher energy, and such a transition is observed earlier in selenides relative to sulfides.

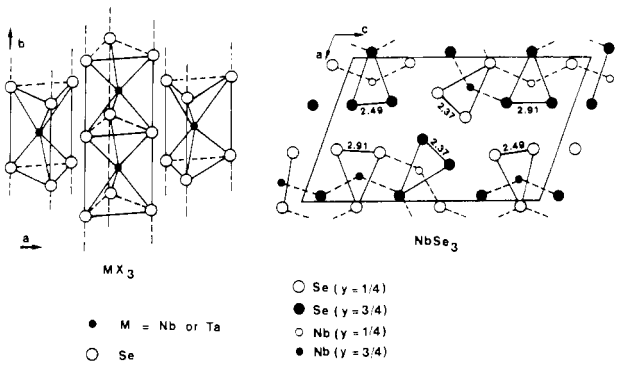

Figure 2. $NbSe_3$ chains parallel to the *b*-axis and their projection onto the *ab*-plane, in the structure of $NbSe_3$. Left, the two-dimensional arrangement.

Chainlike Niobium and Tantalum Trichalcogenides

Crystals of $NbSe_3$ were isolated in the course of a study of the chalcogen-rich side Nb–Se system.[7] Ir-

(5) Fouassier, C.; Delmas, C.; Hagenmuller, P. *Mater. Sci. Eng.* **1977**, *31*, 97.

(6) Piffard, Y.; Verbaere, A.; Lachgar, A.; Deniard, S.; Tournoux, M. *Rev. Chim. Miner.* **1986**, *23*, 766. Crosnier, M. P.; Guyomard, D.; Verbaere, A.; Piffard, Y. *Eur. J. Solid State Inorg. Chem.* **1989**, *26*, 529.

(7) Meerschaut, A.; Rouxel, J. *J. Less-Common Met.* **1975**, *39*, 197.

regular [MX_3] chains, with a chalcogen–chalcogen bond in their triangular basis, run parallel to the *b*-axis of a monoclinic unit cell (Figure 2). Three types of chains with three different values of Se–Se bond lengths (2.37, 2.49, 2.91 Å, respectively[8]) are observed. The two nearest neighboring chains are shifted by $b/2$. $NbSe_3$ shows two charge density waves at 145 and 59 K.[9] It is very likely the most important model compound as far as charge density wave studies are concerned.

Charge density waves (CDWs) are electronic density modulations that occur in low-dimensional conductors when the temperature is decreased, as predicted by Overhauser.[10] In one-dimensional compounds, the CDW modulations are often referred to as Peierls distortions. These instabilities are due to the particular shape of the Fermi surface (FS), i.e., a surface with large parallel sections (nesting condition for low-dimensional conductors). Detailed descriptions are given in the books cited in refs 1–3. The important point, for the purpose of this paper, is that CDWs are a powerful tool, useful in verifying the real dimensionality of a given compound. They have also suggested new syntheses. The main features of CDWs are the following.

(i) The electronic density at a point represented by a vector position **r** along a metallic chain can be written as

$$\rho(r) = \rho_0[1 + \alpha \cos(\mathbf{q}\cdot\mathbf{r} + \phi)]$$

where ρ_0 is the average electronic density before the oscillation, **q** is the wave vector, $\alpha\rho_0$ is the charge modulation amplitude, and ϕ is the phase, which indicates the position of the CDW with respect to the ions of the lattice.

(ii) The metal cations are simultaneously displaced toward the maximum electronic density in order to minimize the energy. Both the charge density and the lattice are periodically modulated with modulation wave vector **q**. The resultant superlattice periodicity can be incommensurate with the initial sublattice, since the **q** vector is fixed by the FS ($\mathbf{q} = 2k_F$).

(iii) Fermi surface is destroyed for those portions satisfying the nesting condition (strong increase in resistivity in $NbSe_3$, metal to insulator transition in perfect 1D conductors). An energy gap opens at the Fermi level, the direct consequence of which is to lower the energy of occupied levels and to raise the energy of unoccupied levels, leading to a gain in electronic energy that compensates for the cost in energy related to the structural distortion.

The above is a static description of a CDW. A new feature identified in $NbSe_3$ is the possible depinning of the CDW.[11] Above a threshold field, nonlinear effects attributed to a collective motion of the CDW are observed.

The $NbSe_3$ chains resemble a direct, one-dimensional transposition of the two-dimensional $NbSe_2$ structure; trigonal prisms are stacked one on top of another instead of arranged in layers. Depending on their lengths, the Se–Se pairs have different electron populations in their antibonding states, i.e., they donate to or accept from the adjacent metallic chains varying amounts of electron density. The 2.374 (4) Å distance is quite typical of an $(Se_2)^{2-}$ pair. Niobium possesses a d^1 configuration, and the chain is therefore represented by the formula $Nb^{4+}Se^{2-}(Se_2)^{2-}$. Larger values of the Se–Se bond lengths correspond to a depletion of the electron density around niobium or a lowering of the population of the conduction band, which is built up by overlapping d_{z^2} orbitals along the chains. The Se–Se pairs behave as electron reservoirs, controlling the electronic properties of the niobium chains. The two CDW are localized on the two chains exhibiting the two shortest Se–Se bond lengths. This conclusion is deduced from the superstructures that are observed below the CDW transitions and that can be clearly related to the internal characteristics and relative orientations of the chains.

Niobium trisulfide (NbS_3), relative to the first type of $NbSe_3$ chain, contains the same [MX_3] trigonal prismatic framework, $(S–S)^{2-}$ pairs ($D_{s\text{-}vps}$ = 2.050 (8) Å), and niobium in a formal 4+ oxidation state or a d^1 configuration. The lone electron, however, is not delocalized along the chain. A d^1–d^1 pairing, which implies an alternation of long and short Nb–Nb distances[12] and which results in a superstructure with a doubling of the period in the chain direction, is observed. This interaction can be regarded as the insulating state of a CDW transition occurring at higher temperatures. When heated, NbS_3 approaches this transition (the superlattice rows of spots in a Bragg pattern are changed into diffuse lines that announce the transition), but the compound decomposes before it is fully achieved.

$NbSe_3$ is not a perfect 1D conductor because it remains metallic below the CDW transitions, indicating that only a portion of the Fermi surface is nested. Vibrational studies show a rather strong interaction between a given atom and selenium atoms of the neighboring chains. This interchain coupling prompts a modification of the simple d-sp redox model (mentioned above) to include the three-chain interactions.[13] As previously stated in the preliminary remarks, success in the preparation of a more one-dimensional material is dependent upon an increase in the ionicity of the metal–chalcogen bonds (NbS_3 versus $NbSe_3$). Tantalum trisulfide, an analogous compound, contains a more electropositive metal and a more electronegative nonmetal than $NbSe_3$. An orthorhombic form of TaS_3,[14] whose detailed structure long remained undetermined, exhibits expected increased one-dimensional character, as revealed by three points.

(i) A complete metal to insulator phase transition occurs at 210 K.[15] FS is completely destroyed, as is expected for a true 1D conductor.

(ii) An important phenomenon, detected by X-ray analysis in the form of diffuse lines between the main rows of Bragg spots, exists far above the CDW transition. These diffuse lines announce the phase transition by eventually coalescing into sharp spots at 210 K. The CDW therefore appears to exist dynamically above the

(8) Hodeau, J. L.; Marezio, M.; Roucau, C.; Ayroles, R.; Meerschaut, A.; Rouxel, J.; Monceau, P. *J. Phys. C: Solid State Phys.* **1978**, *11*, 4117.
(9) Haen, P.; Monceau, P.; Tissier, B.; Waysand, G.; Meerschaut, A.; Molinié, P.; Rouxel, J. *Proc. 14th Int. Conf. Low Temp. Phys.*, Otaniemi, Finland, 1975; North-Holland: Amsterdam, 1975; Vol. 5, p 445.
(10) Overhauser, A. W. *Phys. Rev. B* **1968**, *167*, 691.
(11) Monceau, P.; Ong, N. P.; Portis, A. M.; Meerschaut, A.; Rouxel, J. *Phys. Rev. Lett.* **1976**, *37*, 602.
(12) Rijnsdorp, J.; Jellinek, F. *J. Solid State Chem.* **1978**, *25*, 325.
(13) Hoffmann, R.; Shaik, S.; Scott, J. C.; Whangbo, M. H.; Foshee, M. J. *J. Solid State Chem.* **1980**, *34*, 263.
(14) Bjerkelund, E.; Kjekshus, A. *Z. Anorg. Allg. Chem.* **1964**, *B328*, 235.
(15) Sambongi, T.; Tsutsumi, K.; Shiozaki, Y.; Yamamoto, M.; Yamaya, K.; Abe, Y. *Solid State Commun.* **1977**, *22*, 729.

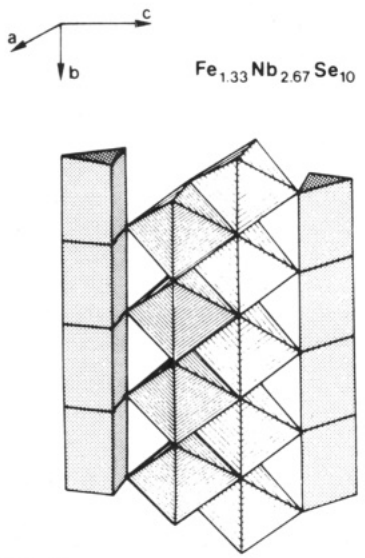

Figure 3. $FeNb_3Se_{10}$ structure.

transition, but without phase coherence from one chain to another. In the case of $NbSe_3$, similar diffuse lines are very difficult to observe.[16]

(iii) Increased one-dimensional character allows the chains to behave more and more as independent units. This is one reason, among others, why polytypes are often encountered in low-dimensional materials (1D structures are no exception). The chains should be able to associate with like or similar chains in various arrangements. Polytypes of $NbSe_3$ have never been observed, but tantalum trisulfide has a monoclinic phase in addition to the orthorhombic one. Each structure is derived from a different arrangement of three types of chains (chains with 2.835 (3), 2.105 (4), and 2.068 (3) Å S–S distances are present, the latter one corresponding to a true $(S–S)^{2-}$ pair). The *b* monoclinic axis is equal to the *c* orthorhombic one. Both characterize the height of one $[TaS_6]$ prism (see ref 3, p 231).

Low-Dimensional Compounds from the Condensation of Different Chains or the Segregation of Chains in a Framework with a Higher Dimensionality

Limited amounts of other atoms can be substituted for niobium in $NbSe_3$ since the chain imposes the trigonal prismatic symmetry on the substituents. They introduce a random potential along the chains and influence the depinning threshold field of CDWs. For larger amounts of foreign metals, phase separation occurs because each element tends to adopt its preferred coordination.

The compound $FeNb_3Se_{10}$ was thus obtained by direct combination of the elements at 650 °C in evacuated silica tubes.[17–19] Trigonal prismatic coordination, expected for niobium, would have been very uncommon for iron; indeed, a segregation of the metallic components into two types of chains,[18,19] associated two by two and running along the *b*-axis of monoclinic unit cell, is observed (Figure 3). The first consists of a trigonal prismatic framework of selenium atoms around one set of niobium atoms. The other chain is comprised of an octahedral arrangement of selenium atoms around both iron atoms and a second set of niobium atoms. A variation of the Fe/Nb ratio in the octahedral chains accounts for deviations from the stoichiometric formulation, which should be replaced by the expression $Fe_{1+x}Nb_{3-x}Se_{10}$ $(0.25 < x < 0.40)$. The trigonal prismatic chain exhibits a short Se–Se bond length of 2.348 (1) Å, which is very close to the length of the shortest Se–Se bond in $NbSe_3$. A metal to nonmetal transition is observed at approximately 140 K. Superlattice spots appear below the transition and characterize a distortion whose wave vector components are similar to those of the first CDW in $NbSe_3$. This result seems to indicate that the distortion is localized within the chain that is common to both compounds. It is also, to some extent, a "chemical" characterization of the chain bearing the CDW. The random potential created by the disordered, adjacent Fe–Nb octahedral chain may explain why an insulating state is achieved in the case of $FeNb_3Se_{10}$.

The structure of $FeNb_3Se_{10}$ may be considered as the result of condensations (within a given structure type) of various chains, each containing the usual coordination for a given metal. This concept of multichain condensations is also illustrated by phases containing trigonal prismatic, square planar ($Nb_2Pd_3Se_8$[20]), or tetrahedral chains (Ta_2NiS_5[21]).

Chain condensations lead to the preparation of sheets ($FeNb_3Se_{10}$) or even three-dimensional structures ($Nb_2Pd_3Se_8$). The end point is a material possessing increased bonding dimensionality, even though specific physical properties may retain 1D character.

Stabilization of Chains by Counterions: Halogenotetrachalcogenides

The structure of the mineral patronite, VS_4, is well known[22] and is characterized by the presence of individual $[VS_4]$ chains in which $(S_2)^{2-}$ pairs form S_4 rectangles that rotate around a vanadium chain to give a rectangular antiprismatic coordination about the metal atoms. Long and short vanadium–vanadium distances alternate along the chains. The lone d electron on V^{4+} is used in the formation of V–V pairs. Consequently, VS_4 is a diamagnetic semiconductor.

Attempts to prepare NbS_4 or TaS_4 have been unsuccessful, probably due to a relatively high bond ionicity which destabilizes the one-dimensional arrangement. Even $NbSe_4$ and $TaSe_4$ are unstable, in spite of a lower bond ionicity. In fact, only tetratellurides are stable. They show a complicated modulated variant of the VS_4 structure.[23–25] Addition of iodine to mixtures of the elements at 500 °C in evacuated, sealed glass tubes, on the other hand, produces single crystals of a new series of phases with the general formula $(MSe_4)_nI$ (M = Nb, Ta; n = 2, 3, $^{10}/_3$, ...).[26–28]

(16) Pouget, J. P.; Moret, R.; Meerschaut, A.; Guémas, L.; Rouxel, J. *J. Phys., Colloq.* **1983**, *44*, (Suppl. No. 6), C3-1729.
(17) Hillenius, S. H.; Coleman, R. V.; Fleming, R. M.; Cava, R. J. *Phys. Rev. B* **1981**, *23* (5), 1567.
(18) Cava, R. J.; Hines, V. L.; Mighell, A. D.; Roth, R. S. *Phys. Rev. B* **1981**, *24* (6), 3634.
(19) Meerschaut, A.; Gressier, P.; Guémas, L.; Rouxel, J. *Mater. Res. Bull.* **1981**, *16*, 1035.
(20) Kezsler, D. A.; Ibers, J. A. *Inorg. Chem.* **1985**, *24*, 3611.
(21) Sunshine, S. A.; Ibers, J. A. *Inorg. Chem.* **1985**, *24*, 3611.
(22) Allman, R.; Bauman, L.; Kutoglu, A.; Rösch, H.; Hellner, E. *Naturwissenschaften* **1964**, *51*, 263.
(23) Selte, K.; Kjekshus, A. *Acta Chem. Scand. Ser. A* **1960**, *18*, 690.
(24) Böhn, H.; Von Schnering, H. G. *Z. Kristallogr.* **1983**, *162*, 26.
(25) van Smaalen, S.; Bronsema, K. D. *Acta Crystallogr., Sect. B* **1986**, *42*, 43.
(26) Meerschaut, A.; Palvadeau, P.; Rouxel, J. *J. Solid State Chem.* **1977**, *20*, 21.

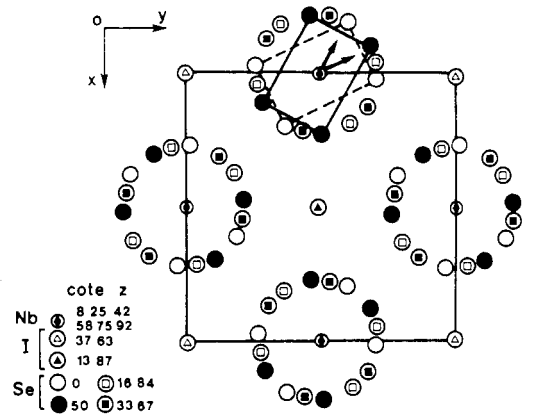

Figure 4. Projection of MX_4 chains and counterion columns of halogenotetrachalcogenides onto the basal plane of the tetragonal unit cell (see also Figure 6).

Needle-shaped crystals of $(NbSe_4)_3I$ crystallize in a tetragonal symmetry (space group $P4/mnc$). The structure (Figure 4) is composed of $[NbSe_4]$ chains aligned along the c-axis and separated by columns of iodine. The niobium coordination, consisting of true selenide pairs (d_{Se-Se} = 2.37 (1) Å), is in the form of a rectangular antiprism like that observed in VS_4. Along the metallic chains, one short (3.06 Å) and two long (3.25 Å) Nb–Nb distances alternate. This sequence changes from one compound to another according to the concentration of the counterion. Another variable concerns the way in which $[Se_4]^{4-}$ rectangles rotate about the metallic chain. Any two successive rectangles are rotated by an angle of 45°, which minimizes the energy of an $[MSe_8]$ "molecular group" (the repulsion between occupied π and π^* orbitals is minimized, and the best set of symmetry-adapted orbitals to interact with the metal orbitals is obtained). The relative displacement of successive rectangles corresponds to a right- or left-handed rotation that can be described with the help of arrows pointing toward the middle of an Se–Se pair. Thus, $(NbSe_4)_3I$, $(TaSe_4)I$, and $(NbSe_4)_{10/3}I$ are 123432, 1234, and 1234565432 tetrachalcogenides, respectively.[29] All of the metal orbitals, with the exception of the d_{z^2} orbitals, contribute to the bonding in the MSe fragment. The remaining d_{z^2} orbitals bond along the chain and form a band that governs the electronic properties of the system. Given d^1 systems (e.g., Nb^{4+}, Ta^{4+}) and assuming each iodine takes one electron, then the average number of remaining d electrons per metal is $(n - 1)/n$, corresponding to a filling of the d_{z^2} band equal to $(n - 1)/2n$. This approach allows one to predict the distortions that may possibly occur. For example, $(TaSe_4)_2I$[30,31] and $(NbSe_4)_{10}I_3$[32] exhibit CDW transitions at 263 and 285 K, respectively. Depinning experiments have been successfully attempted. In addition, $(NbSe_4)_{10}I_3$ exhibits hysteresis between 220 and 285 K, implying one threshold field when the applied field is increased and another when it is decreased.[32]

As n increases, the d_{z^2} band of $(MSe_4)_nI$ becomes close to half-filled. Vanadium tetrasulfide constitutes an example of the $n \rightarrow \infty$ limit. It has a $2c$ superstructure along the chain direction in the form of V–V pairs (d^1–d^1 pairing) alternating with longer distances. Physically, this insulating state is a true Peierls distortion. A gap is created in the conduction band at the Fermi level, lowering the energy of the occupied states (metal–metal bonding) and raising the energy of the unoccupied states (antibonding levels).

Condensation of Various Structural Units and Stabilization of Chains by Other Chains

The tetrachalcohalogenides were first obtained in the case of iodine. Attempts to prepare the bromine and chlorine homologues have been largely unsuccessful. Only a few poorly crystalline bromine compounds have been obtained.[33] This is, once again, a consequence of the increased ionic character of the compounds resulting from the substitution of a more electronegative halogen. Furthermore, the smaller size of the halogen does not minimize the interchain repulsions by sufficiently separating the chains.

A more electronegative halogen, in fact, tends to participate directly in the coordination polyhedra of the metal by displacing the selenium framework. In addition to the phases containing $(Se_4)_2$ rectangular antiprismatic coordination, phases in which niobium atoms are directly bonded to the halogen are formed. A better description is to consider these compounds to be based on structural units of $[M_2X_4]$ bipyramids: two metal atoms on each side of an X_4 rectangle. This approach permits a general classification that includes the tetrahalogenochalcogenides and other related phases. Compounds like $Nb_6Se_{20}Br_6$,[34] which possesses a waved structure (Figure 5), and $M_4Se_{16}Br_2$ (M = Nb, Ta)[35] then appear to result from a partial condensation of $[Nb_3Se_9]$ and $[Nb_4Se_{12}]$ bipyramidal groups separated by halogen-bonded niobium atoms. The same bipyramids are found isolated in Nb_2Se_9[36] and in $Nb(S/Se)_2Cl_2$,[37] where they are separated by Se_5 groups or Cl^-, respectively (Figure 6). On the other hand, they give rise to an infinite condensation in VS_4, where the (MX_4) chains are completely juxtaposed, or in $(MSe_4)_nI$, where the chains are separated by iodine.

It is clear that the $(NbSe_4)$ or $(TaSe_4)$ chains could be stabilized by many counterions other than I^-, provided certain charge and size conditions were satisfied. Another approach is the preparation of mixed-chain compounds, i.e., materials containing two different types of chains. An example is the compound $Nb_3Se_{10}Br_2$,[38] whose structure is composed of alternating $(NbSe_4)$ chains centered along a 2-fold axis and $(NbSe_3Br)$ chains running along a parallel 2_1 axis (Se–Br

(27) Gressier, P.; Meerschaut, A.; Guémas, L.; Rouxel, J.; Monceau, P. *J. Solid State Chem.* **1984**, *51*, 141.
(28) Fujishita, H.; Sato, M.; Hoshino, S. *Solid State Commun.* **1984**, *49*, 313.
(29) Gressier, P.; Whangbo, M. H.; Meerschaut, A.; Rouxel, J. *Inorg. Chem.* **1984**, *23*, 1221.
(30) Wang, Z. Z.; Saint Lager, M. C.; Monceau, P.; Renard, M.; Gressier, P.; Meerschaut, A.; Guémas, L.; Rouxel, J. *Solid State Commun.* **1983**, *16*, 325.
(31) Maki, M.; Kaiser, M.; Zettl, A.; Grüner, G. *Solid State Commun.* **1983**, *46*, 497.
(32) Wang, Z. Z.; Monceau, P.; Renard, M.; Gressier, P.; Guémas, L.; Meerschaut, A. *Solid State Commun.* **1983**, *47* (6), 439.
(33) Guémas, L.; Gressier, P.; Meerschaut, A.; Loüer, D.; Grandjean, D. *Rev. Chim. Miner.* **1981**, *18*, 91.
(34) Meerschaut, A.; Grenouilleau, P.; Rouxel, J. *J. Solid State Chem.* **1986**, *61*, 90.
(35) Grenouilleau, P.; Meerschaut, A.; Guémas, L.; Rouxel, J. *J. Solid State Chem.* **1987**, *66*, 293.
(36) Meerschaut, A.; Guémas, L.; Berger, R.; Rouxel, J. *Acta Crystallogr., Sect. B* **1979**, *35*, 1747.
(37) von Schnering, H. G.; Beckmann, W. *Z. Anorg. Allg. Chem.* **1966**, *347*, 231. Rijnsdorp, J.; Delange, G. J.; Wiegers, G. A. *J. Solid State Chem.* **1979**, *30*, 365.
(38) Meerschaut, A.; Grenouilleau, P.; Guémas, L.; Rouxel, J. *J. Solid State Chem.* **1987**, *70*, 36.

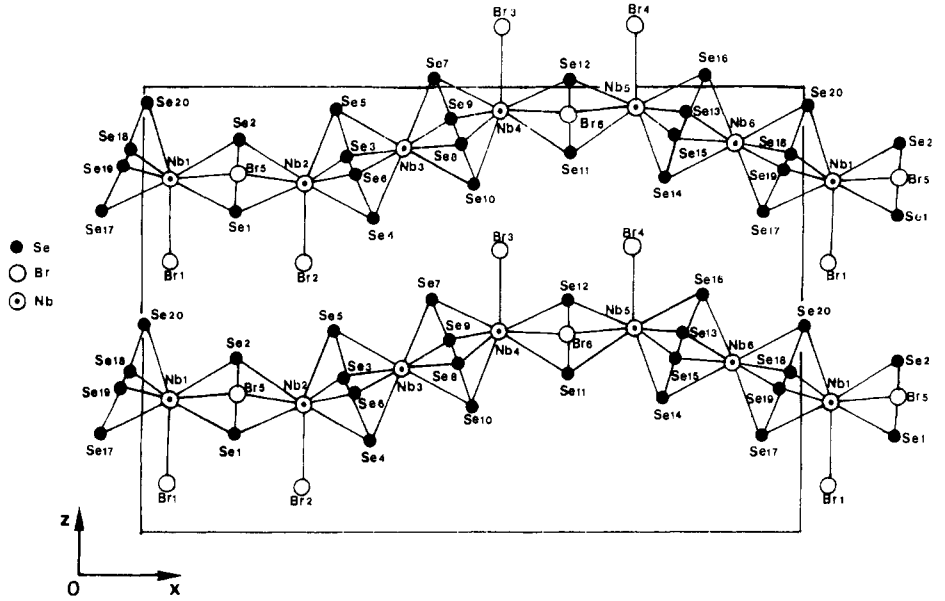

Figure 5. $Nb_6Se_{20}Br_6$ structure. Pieces of MX_4 chains (around Nb_3 and Nb_6) alternate with Nb atoms having Br neighbors.

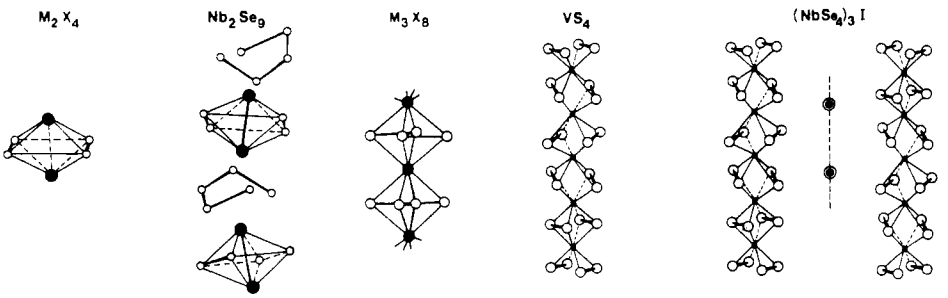

Figure 6. Partial or infinite condensation of M_2X_4 bipyramids [e.g., Nb_2Se_9 with isolated bypyramids, $[M_3X_8]$ groups of two bipyramids in $Nb_6Se_{20}Br_6$ represented in Figure 5, $(NbSe_4)_nI$ and VS_4 with an infinite condensation].

exchange on particular sites explains the rather complicated formulation).

In order to test the above hypothesis on the preparation of mixed-chain compounds, reactions between one-dimensional compounds requiring counterions of opposite charge for their stabilization[39] were designed. $(Nb–Ta)Se_4I_n$ phases were allowed to react with $(Mo_6Se_6)A_2$ compounds, which contain Mo_6Se_6 chains stabilized by A^+ counter cations (A = alkali metal or thallium).[40] Solid-state syntheses, as well as reactions with colloidal dispersions of Mo_6Se_6 chains,[41] have been attempted. Along with the formation of the byproduct salt AI, a $[(Ta–Nb)Se_4]_m(Mo_6Se_6)_n$ compound was expected. All of the trials, however, were unsuccessful. At this point, $Nb_3Se_{10}Br_2$ seems to be the only compound of that type. The above examples prove that the concept is correct but that the interchain interactions have to be defined before synthetic strategies can be designed.

Multilayer Fibers

Complex layered structures in which the slabs involve more than three-layered [XTX] sandwiches of transition-metal chalcogenides have long been recognized. For example, Bi_2Te_3 is composed of five-layer Te–Bi–Te–Bi–Te slabs (Figure 7). Tantalum carbosulfide, an

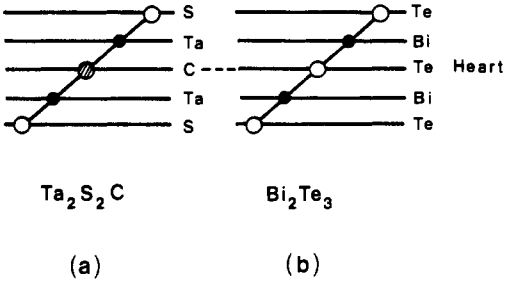

Figure 7. Five-layer slabs of Ta_2S_2C (a) and Bi_2Te_3 (b).

analogous compound containing five-layer sheets of [S–Ta–C–Ta–S],[42] is structurally related to semimetallic transition-metal insertion compounds as well as to ionic/covalent materials. If the single tantalum layer in TaS_2 is replaced by a [Ta–C–Ta] sandwich, tantalum carbosulfide is obtained. Similarly, the new compound Ta_4SiTe_4[43] can, in a certain sense, be considered a unidimensional analogue of Ta_2S_2C. Instead of a carbon layer, it contains a central Si chain or backbone surrounded by a repeating sequence of atomic layers. Si-centered chains of antiprismatically stacked tantalum squares are edge-bridged by tellurium atoms. Figure 8 illustrates these 4-fold symmetric chains. The nearest-neighbor Te–Te interchain distances range from 3.815 to 3.830 Å, typical of van der Waals bonding between tellurium atoms. Ta_4SiTe_4 is a true one-dimen-

(39) Guêmas, L.; Meerschaut, A.; Rouxel, J. Unpublished results.
(40) Potel, M.; Chevrel, R.; Sergent, M. *Acta Crystallogr., Sect. B* **1980**, *36*, 1545.
(41) Tarascon, J. M.; di Salvo, F. J.; Chen, C. H.; Corroll, P. J.; Walsh, M.; Rupp, L. *J. Solid State Chem.* **1985**, *58*, 290.
(42) Beckmann, O.; Boller, H.; Nowstny, H. *Monatsh. Chem.* **1970**, *101*, 945.
(43) DiSalvo, F. J. *Science* **1990**, *247*, 649.

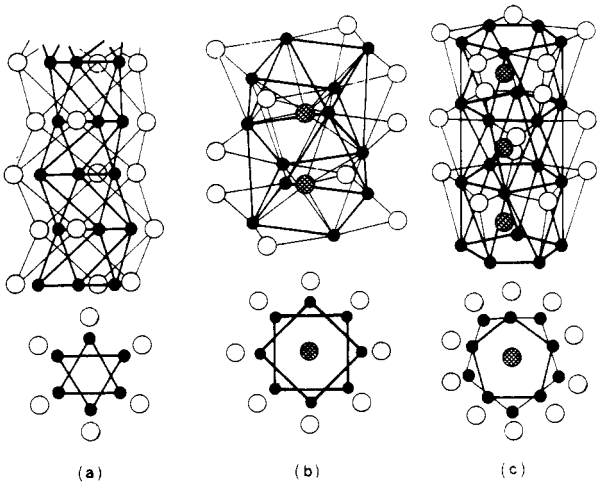

Figure 8. Trigonal antiprismatic chains in $A_2Mo_6Se_6$ (a); Ta_4SiTe_4 chains (b). Square antiprisms of tantalum atoms form a chain which is Si-centered and edge-bridged by Te. Ta_5TaS_5 chains isolated from the structures of metal-rich tantalum sulfides (c) (Ta_5TaS_5 does not exist by itself). The pentagonal antiprismatic chains of Ta atoms are centered by a Ta chain.

sional compound. This compound is particularly important for two reasons. First, it is just one member of a class of isostructural compounds with the general formula Ta_4ZTe_4, where Z = Cr, Fe, Co, Ni, Al, and Si.[44] Second, niobium seems to form an analogous class of compounds. This new type of chain compound possesses a 4-fold symmetry. One-dimensional compounds containing chains of 3-fold or 5-fold symmetry are also known. The structure of $InMo_3Te_3$,[45] for example, consists of infinite chains of triangular Mo_3 monomers, edge-bridged by Te and stacked antiprismatically to form a one-dimensional metal atom network. The difference between $InMo_3Te_3$ and Ta_4SiTe_4 is that the chains are not centered by any extra atom. The indium atoms are actually found between the chains. This is a case of chain stabilization by counter cations. The chains are formally a 3-fold symmetry transposition of the Ta_4Te_4 framework in Ta_4SiTe_4. Pentagonal antiprismatic chains of Ta_5TaS_5 have been characterized as the common structural building blocks in tantalum-rich sulfides such as Ta_6S and Ta_2S[46-48] or Ta_3S_2.[48,49] These phases are members of the Ta_6S_n series (Ta_6S, Ta_6S_3, and Ta_6S_4, respectively). The Ta_6S_5 chains result from a stacking of Ta_5 pentagons in a staggered fashion. Extra tantalum atoms are present in the centers of the pentagonal antiprisms, and external sulfur atoms cap alternate, exposed, triangular chain faces (Figure 8). The structural formulation, Ta_5TaS_5, expresses quite well the similarity with Ta_4SiTe_4. An important difference is that the structural units are not independent, intact chains. This is likely a consequence, once again, of an elevated bond ionicity (remember "NbS_4" and $NbTe_4$). The Ta_6S_n structure may be the result of various modes of lateral chain condensations with sulfur elimination to form, for example, a two-dimensional Ta–Ta network in Ta_6S_4 and a three-dimensional one in Ta_6S_3 (more sulfur is eliminated).

Mixed-Polyhedra, "Supermolecular" Architectures

The complex slabs of layered silicates, incorporating octahedra and tetrahedra, have already been cited in the introduction, along with the similar phosphato-antimonates and related phases. In the field of chain-like materials, fascinating compounds associating two types of polyhedra have been prepared in the V–P–S, Nb–P–S, and Ta–P–S systems. The two types of polyhedra can either alternate within the same chain or one type can connect chains that are composed exclusively of the other.

Layered phases are well known in the M–P–S systems, where M is a transition element.[50] These compounds are the MPS_3 phases, which contain slabs similar to those of TiS_2 except that the octahedra are occupied by M^{2+} cations and P–P pairs in the ratio of 2/3 to 1/3. The formulation of a slab is, therefore, $[S{M^{2+}}_{2/3}(P_2)_{1/3}S]$. The new phases, obtained on the chalcogen-rich side of these systems, exhibit one-dimensional character. As will be explained below, they are not simple, structural, one-dimensional transpositions of two-dimensional arrangements, like $NbSe_3$ relative to $NbSe_2$.

All of these phases contain the same basic structural unit, a tetracapped biprism of $[M_2S_{12}]$ (Figure 9a). The biprisms, via edge-sharing, are linked in infinite $[M_2S_9]$ chains (Figure 9b). Finally, $[PS_4]$ tetrahedra in capping positions connect the chains via the sulfur atoms. The manner in which such bonding occurs determines the dimensionality of the system. $[P_2S_8]$ or $[P_2S_9]$ groups, $S_3P(-S-S-)PS_3$ or $S_3P(-S-S-S-)PS_3$ linkages, respectively, are found between the chains. For example, PV_2S_{10}[51] is a 1D compound of $[M_2S_9]$ chains connected two by two by $[P_2S_8]$ groups. On the other hand, PNb_2S_{10}[52] is a 2D compound with $[P_2S_8]$ groups joining the chains on both sides. Longer $[P_2S_9]$ groups insure a step-linking of the chains in the 2D $P_2Nb_4S_{21}$.[53]

When the biprisms do not form $[M_2S_9]$ chains but are directly connected to each other by the $[PS_4]$ tetrahedra, intriguing new structural types containing tunnels formed by complicated helicoidal chains are observed. $Ta_4P_4S_{29}$ is probably the most typical, as well as the most fascinating, of these compounds.[54] In this particular structure, $[Ta_2S_{12}]$ biprisms are connected by single $[PS_4]$ tetrahedra that join the upper corner of one biprism to the lower corner of the adjacent biprism (Figure 10). The resulting helical configuration has four biprisms per repeat distance and can be either right-handed or left-handed. The structure contains yet another helix, a right-handed sulfur S_{10} helical chain. Each unit cell is composed of two large, intertwined, right-handed helices and two small, left-handed helices that combine to produce small empty tunnels. These results come from a refinement carried out in the space

(44) Badding, M. E.; DiSalvo, F. J. *Inorg. Chem.*, in press. Corbett, J.; et al. Manuscript in preparation.
(45) Honle, W.; Von Schnering, H. G.; Lipka, A.; Yvon, K. *J. Less-Common Met.* **1980**, *71*, 135.
(46) Franzen, H. F.; Smeggil, J. G. *Acta Crystallogr.* **1969**, *B25*, 1736.
(47) Franzen, H. F.; Smeggil, J. G. *Acta Crystallogr.* **1979**, *B26*, 125.
(48) Harbrecht, B. *J. Less-Common. Met.* **1979**, *138*, 225. Kim Sung-Jin; Nanjundaswamy, K. S.; Hughbanks, T. Manuscript in preparation.
(49) Hughbanks, T. *Prog. Solid State Chem.* **1989**, *19*, 329.
(50) Hahn, H.; Klinger, W. *Naturwissenschaften* **1965**, *52*, 494.
(51) Brec, R.; Ouvrard, G.; Evain, M.; Grenouilleau, P.; Rouxel, J. *J. Solid State Chem.* **1987**, *7*, 244.
(52) Brec, R.; Grenouilleau, P.; Evain, M.; Rouxel, J. *Rev. Chim. Miner.* **1983**, *20*, 295.
(53) Brec, R.; Evain, M.; Grenouilleau, P.; Rouxel, J. *Rev. Chim. Miner.* **1983**, *20*, 283.
(54) Evain, M.; Queignec, M.; Brec, R.; Rouxel, J. *J. Solid State Chem.* **1985**, *56*, 148.

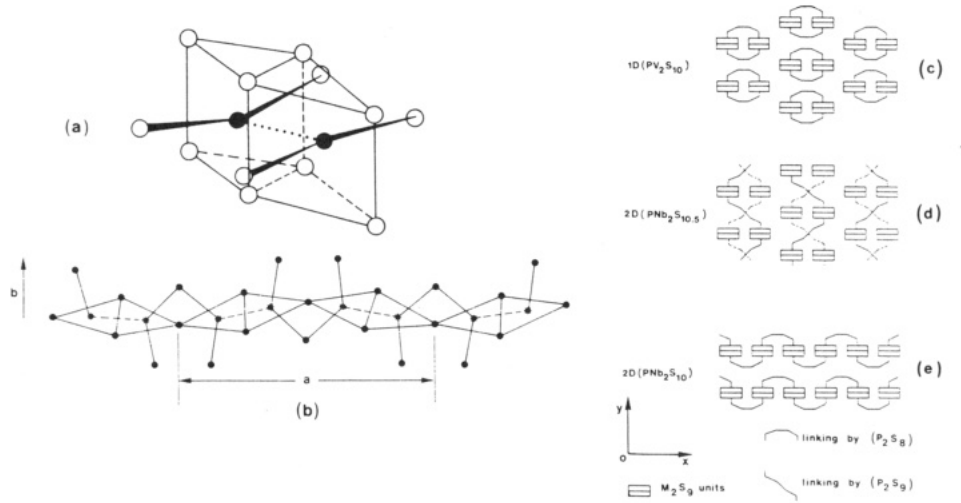

Figure 9. M_2S_{12} bicapped biprism (a), formation of $(M_2S_9)_\infty$ chains from M_2S_{12} biprisms (b) and association of these chains by P_2S_8 and P_2S_9 groups in 1D PV_2S_{10} (c), 2D $P_2Nb_4S_{12}$ (d), and 2D PNb_2S_{10} (e).

group $P4_32_12$. Refinement in the $P4_12_12$ space group, which corresponds to a structure based on large left-handed and small right-handed helices, yielded a worse result with the same crystal. It is clear, however, that the left-handed form very likely exists. The compounds $P_2Nb_2S_8$, $Ta_2P_2S_{11}$, and $V_2P_4S_{13}$ are likewise composed of $[M_2S_{12}]$ biprisms directly linked by $[PS_4]$ tetrahedra. A complete description is found in ref 55.

Conclusions and Summary

A careful inspection of known phases has led to a number of general conclusions on the synthesis of low-dimensional materials. The guidelines, however, are quite qualitative since they only provide the researcher with a feeling for (and not the exact numbers concerning) low-dimensional compounds. Nevertheless, they allow one to identify where, in the field of chemistry, the harvest of low-dimensional compounds is the best. The chemistry of niobium and tantalum is one of these domains. Simple chain arrangements are found in tri- and tetrachalcogenides. In the latter case, only telluride chains exist independently; selenide chains have to be stabilized by counterions or -chains. More complex structures are based on (i) the condensation of different chains ($FeNb_3Se_{10}$), (ii) 1D intergrowth of different units (Nb_6Se_6Br), or (iii) multicomponent fibers (Ta_4SiTe_4). The intriguing structures of P–(Nb–Ta)–S phases are based on a supermolecular architecture associating at least two different types of coordination polyhedra. $Ta_4P_4S_{29}$, with double intertwined helices, is a remarkable example.

Even if a structure is crystallographically two-dimensional, it may only be unidimensional with respect to a certain physical property. This behavior, exemplified in $FeNb_3Se_{10}$, is also present in the so-called blue bronze $K_{0.30}MoO_3$[56] (covalent Mo–O bonds result in two-dimensional MoO_3 sheets, although the conduction band formed from Mo d and O p orbitals has a one-dimensional character).

These new solids are generally metastable phases, which on heating transform to stable compounds (chalcogenides with a lower chalcogen content, poly-

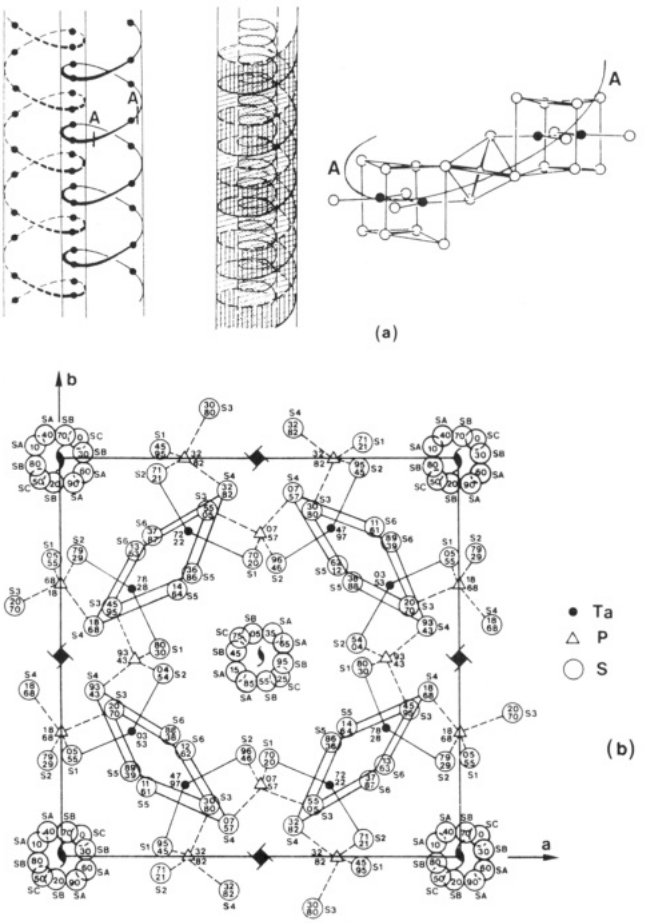

Figure 10. M_2S_{12} biprisms connected by PS_4 tetrahedra (right) to form intertwined helices (left), each containing a sulfur helix (a). Projection of the $Ta_4P_4S_{29}$ structure onto a plane perpendicular to the direction of the helix, showing the sulfur helix inside the layer one (b).

types, or a mixture of stable phases). As a consequence, syntheses are often conducted at low to medium temperatures (350–600 °C) in sealed, evacuated glass or silica tubes, i.e., under thermodynamic conditions that are difficult to evaluate. Series of compounds are often obtained which differ only slightly from each other—$(MX_4)_nI$ phases, for example. Different crystals corresponding to different values of n may be obtained in the same tube. A specific compound is associated with

(55) Evain, M.; Brec, R.; Whangbo, M. H. *J. Solid State Chem.* **1987**, *71*, 244.
(56) Wold, A.; Kunmann, W.; Arnott, R. J.; Feretti, A. *Inorg. Chem.* **1964**, *3*, 545.

a narrow temperature range and particular starting conditions, such as tube volume and reactant quantities. Each crystal must, nevertheless, be fully characterized, particularly when polytypes exist (TaS_3 case). In addition, the closely related structures of the various phases make intergrowth phenomena likely. Intergrowth would lead to slight local displacements of metal and iodine atoms in their respective chains. Chain fragments of one type in another can strongly influence the depinning energy of CDWs in $NbSe_3$, although the role of chemical impurities has recently been recognized as being very important.[57]

The chemistry of low-dimensional solids is a particularly fertile domain, as is often the case for interdisciplinary fields. It illustrates the importance of ties that exist between coordination chemistry and the solid state.[58] The close relationship is manifested in remarkable similarities in terms of structures, orbital descriptions, and unusual physical properties (i.e., charge density waves, spin density waves, and low-dimensional magnetism). These similarities give one the impression that there is some underlying principle unifying the two fields. This approach, however, should not be developed beyond what is supported by experimental results.

This work was made possible thanks to the contributions of many outstanding colleagues and graduate students. I would especially like to acknowledge A. Meerschaut, R. Brec, M. Evain, L. Guemas, and P. Gressier, who work with me in Nantes, and M. Whangbo of the University of North Carolina at Raleigh, who spent some time here as a visiting professor.

(57) Thorn, R.; Cornell U. Personal communication.

(58) Sunshine, S. A.; Keszler, D. A.; Ibers, J. A. *Acc. Chem. Res.* **1987**, *20*, 395-400.

Polyelectrolyte-Sensitized Phospholipid Vesicles

JAMES L. THOMAS and DAVID A. TIRRELL*

Department of Polymer Science and Engineering, University of Massachusetts, Amherst, Massachusetts 01003

Received January 29, 1992

Control of the structure and permeability of biological membranes is one of the most basic and least understood problems in contemporary biophysics. Diverse cellular processes require exquisite control of the membrane structure, including endocytosis and exocytosis, maintenance of the Golgi apparatus and the endoplasmic reticulum, and mitosis and meiosis, to mention just a few. Recently, significant progress has been made in controlling the permeability, and often the structures, of synthetic bilayer vesicles. These studies are especially important in that they help elucidate previously unimagined mechanisms for membrane control. Although no single model system is likely to utilize all of the rich capabilities exploited in nature, the synthetic systems can serve to identify concepts and mechanisms likely to be useful in a biological context. In addition, control of vesicular membrane systems may usher in novel chemistries for use in imaging, sensing, and therapeutic applications.

Particular attention has been given to the synthesis of vesicles that are responsive to their environment through increased permeability or fuseogenicity, since such vesicles have therapeutic potential as vehicles for targeted drug delivery[1,2] (Figure 1). Environmental cues associated with the target, such as the low pH in an endosome of a cell that has internalized a targeted vesicle, can be used to trigger vesicle permeabilization or fusion with the endosomal membrane. Targeting has been achieved by anchoring antibodies, specific for tumor or viral antigens, to the vesicle surface. Excellent reviews of this application of responsive vesicles have been published by Collins and Huang[3] and by Papahadjopoulos and Gabizon.[4]

pH-sensitive vesicles have also been used as tools for fundamental studies in cell biology. The capability of delivering foreign DNA, RNA, antibodies or other proteins, or fluorescent labels to the cytoplasmic compartment of cultured cells is necessary to gain an understanding of the complex chemistry and organization of the cytoplasm. An important step in the use of pH-sensitive vesicles for these applications has been made by Reddy et al.,[5] who showed that pH-sensitive vesicles could be used to deliver a foreign protein (ovalbumin) to the cellular cytoplasmic compartment more efficiently than osmotic loading, which has conventionally been used to introduce foreign materials into cultured cells. Another important application of pH-sensitive vesicles has been as "microsensors" to determine the kinetics of acidification in cellular endocytic compart-

James L. Thomas was born December 2, 1959, in Akron, Ohio. He attended Stanford University (B.S. Physics, 1982) and Cornell University (Ph.D. Physics, 1991). He is currently employed as a postdoctoral fellow in the Department of Polymer Science and Engineering at the University of Massachusetts at Amherst. His principal research interests are the biophysics of membranes and the conformations and chemistry of membrane-active macromolecules.

David A. Tirrell was born January 10, 1953, in Easton, Pennsylvania. He attended MIT (B.S. Chemistry, 1974) and the University of Massachusetts (Ph.D. Polymer Science and Engineering, 1978), and was a postdoctoral fellow at Kyoto University, Japan, in 1978. He is presently Professor of Polymer Science and Engineering and Director of the Materials Research Laboratory at the University of Massachusetts and Editor of the *Journal of Polymer Science, Part A: Polymer Chemistry*. Professor Tirrell's research interests are in polymer synthesis and bioorganic polymer chemistry.

(1) Gabizon, A.; Papahadjopoulos, D. *Proc. Natl. Acad. Sci. U.S.A.* **1988**, *85*, 6949-6953.
(2) Liu, D.; Huang, L. *Biochim. Biophys. Acta* **1990**, *1022*, 348-354.
(3) Collins, D.; Huang, L. In *Molecular Mechanisms of Membrane Fusion*; Ohki, S., Doyle, D., Flanagan, T., Hui, S., Mayhew, E., Eds.; Plenum Press: New York, 1988; pp 149-161.
(4) Papahadjopoulos, D.; Gabizon, A. In *Horizons in Membrane Biotechnology*; Nicolau, C., Chapman, D., Eds.; Wiley-Liss: New York, 1990; pp 85-93.
(5) Reddy, R.; Zhou, F.; Huang, L.; Carbone, F.; Bevan, M.; Rouse, B. *J. Immunol. Methods*, in press.

0001-4842/92/0125-0336$03.00/0